

Embedding via the Exact Factorization Approach

Lionel Lacombe¹ and Neepta T. Maitra¹

¹*Department of Physics, Rutgers University, Newark, New Jersey 07102, USA*

(Dated: September 18, 2019)

We present a quantum electronic embedding method derived from the exact factorization approach to calculate static properties of a many-electron system. The method is exact in principle but the practical power lies in utilizing input from a low-level calculation on the entire system in a high-level method computed on a small fragment, as in other embedding methods. Here, the exact factorization approach is used to define an embedding Hamiltonian on the fragment. Various Hubbard chain models demonstrate that remarkably accurate ground-state energies are obtained over the full range of weak to strongly correlated systems.

The computational challenge of performing a quantum calculation of a complex many-body system remains a primary motivation in many areas of condensed matter physics and quantum chemistry. Density functional theory is often turned to, due to its relatively favorable system-size scaling, however the limitations of available functional approximations deem it inaccurate for strongly correlated systems. When even DFT gets too expensive for a system of more than a thousand atoms or so, a collection of DFT calculations on subsystems with functionals modified by couplings to the rest of the system can be used [1–4], however such an approach remains inadequate for problems involving strong correlation. Instead, one approach in recent years has been to use some kind of quantum embedding method for calculations on complex systems, where the full system is described as an ensemble of two or more fragments: On the one hand, when the fragments are chosen to be weakly-interacting with each other, the essential idea is that properties of the total system can be obtained by a high level calculation on one modified by input from the other. This can be particularly useful when only part of the system is actually of interest, or is strongly-correlated, but such that its environment affects its behavior, and the idea is to calculate accurately properties of the system of interest without having to compute the full problem accurately. On the other hand, when the entire system is of interest and requires a better description of correlation than provided by density functional approximations, GW, and the like, then the high-level calculation can be done successively on different fragments in a self-consistent way, to get a full description of the entire system from several smaller calculations. In the case of periodic system, a cell of various size is chosen to be computed at high level in the bath of the bulk. Several different approaches have been developed in recent decades; ranging from the basic embedding variable being the Green’s function [5, 6] or directly the self-energy [7], to the density-matrix [8–10] or density [11], as well as density-functional based embeddings [12].

Here, we develop a novel embedding method based on the exact factorization (EF) approach. EF separates the wavefunction into a single correlated product of a marginal and a conditional wavefunction [13–18].

Most of the previous work focused on separating the electronic from the nuclear part of a molecular wave function, providing an “exactification” of the BO approximation: $\Psi(\mathbf{R}_1, \mathbf{R}_2, \dots; \mathbf{r}_1, \mathbf{r}_2, \dots) = \chi(\mathbf{R}_1, \dots)\Phi_{\mathbf{R}_1, \dots}(\mathbf{r}_1, \dots)$ where the marginal, $\chi(\mathbf{R}_1, \dots)$, is the nuclear wave function and $\Phi_{\mathbf{R}_1, \dots}(\mathbf{r}_1, \dots)$ the electronic part parametrized by nuclear coordinates. This approach has been successful for giving insight into effects of electronic-nuclear coupling on dynamics (e.g. Refs. [18, 19]) as well as in deriving practical non-adiabatic quantum-classical methods [20–26]. There have been generalizations in several directions; most notably for the present purposes are the exact single-active electron approach arising from factorizing a purely electronic wavefunction into a one-electron marginal and the rest [15, 27], and the formal generalization to arbitrary many-body non-real-space Hamiltonians [28].

The present work extends the EF approach to a completely new class of applications. In our embedding via the exact factorization (EVEF) approach, we factorize the full electronic wavefunction in Fock space. The idea is to solve the full system with a low-level calculation (e.g. Hartree-Fock (HF)), and use the solution to generate an approximate Hamiltonian for the marginal corresponding to a fragment which is then solved with a high-level method (e.g. exact diagonalization). The fragment is a chosen set of single-particle wavefunctions comprising a basis for the Fock space; for example, these can be selected to be the more strongly-correlated orbitals in the one-electron Hilbert space. We present three levels of EVEF, each increasingly refined, and the sensitivity to the choice of fragment depends on which level is chosen. The more sophisticated level utilizes a self-consistent loop to match a chosen quantity computed from the high-level fragment calculation to that from the low-level full calculation, in the same spirit as density-matrix embedding theory (DMET), for example. The results on different Hubbard systems show that EVEF is able to capture the range of weak and strong correlation in an efficient and accurate way.

The Fock space electronic wavefunction is a function of a sequence of zeros and ones, and, for a space of M single-particle orbitals, its factorization reads:

$$\Psi(\underbrace{n_1, n_2, \dots, n_K}_n, \underbrace{n_{K+1}, \dots, n_M}_m) = \chi(n)\Phi_n(m) \quad (1)$$

with $n_i = \{0, 1\}$ representing the occupation of a spin-orbital. The first K spin-orbitals denote the space chosen for the marginal, $\chi(\underline{n})$, a function of the fragment configuration and $\Phi_{\underline{n}}(\underline{m})$ is the conditional part. The factorization is unique up to an \underline{n} -dependent phase, provided the Partial Norm Condition (PNC),

$$\sum_{\underline{m}} \Phi_{\underline{n}}^*(\underline{m})\Phi_{\underline{n}}(\underline{m}) = 1 \quad (2)$$

is satisfied, adapting the proof of Ref. [16, 18]. Then, it follows that

$$\chi(\underline{n}) = \sqrt{\sum_{m_j=0,1} |\Psi(\underline{n}, \underline{m})|^2} \times (e^{iF(\underline{n})}) \quad (3)$$

(with the sum on m_j going over $K+1$ to M spin-orbitals) where the arbitrary phase factor $e^{iF(\underline{n})}$ represents the so-called gauge freedom of EF. The EF approach then usually proceeds by finding a coupled set of equations for the marginal and conditional factors, which contain terms that exactly account for coupling of the two subsystems. However, at this point we deviate from what is usually done in EF: here we find an equation for χ , that emulates the effect of $\Phi_{\underline{n}}$ without actually ever computing it. This avoids having to solve a numerically challenging non-linear and non-Hermitian equation for the conditional wavefunction [28, 29].

To obtain the equation for $\chi(\underline{n})$, consider first the full Schrödinger equation for Ψ , which involves the full exact Hamiltonian \hat{H} :

$$\sum_{\underline{n}', \underline{m}'} H_{\underline{n}, \underline{m}; \underline{n}', \underline{m}'} \Psi_{\underline{n}', \underline{m}'} = E \Psi_{\underline{n}, \underline{m}} \quad (4)$$

Inserting the factorized form Eq. (1), multiplying on the left by $\Phi_{\underline{n}}^*(\underline{m})$, and summing over \underline{m} gives our Schrödinger-like equation for $\chi(\underline{n})$:

$$\sum_{\underline{n}'} h_{\underline{n}; \underline{n}'} \chi(\underline{n}') = E \chi(\underline{n}) \quad (5)$$

where we have used the PNC Eq. (2) on the right-hand-side, and identified the embedded Hamiltonian

$$h_{\underline{n}; \underline{n}'} \equiv \sum_{\underline{m}', \underline{m}} \Phi_{\underline{n}}^*(\underline{m}) H_{\underline{n}, \underline{m}; \underline{n}', \underline{m}'} \Phi_{\underline{n}'}(\underline{m}') \quad (6)$$

So far, everything is exact, and E could be any eigenvalue of the full Hamiltonian; it need not be the ground-state energy. But, to solve the equation for χ one needs to compute h first which is as hard as the original problem. The practical power of this set-up depends on making an approximation.

Before introducing the approximations, we rewrite our formalism in second quantization as it is the most natural language for dealing with Fock space. Moreover, it will allow us to make an efficient use of Wick's Theorem for

when we do introduce our approximation. To begin, we define the operator $\hat{X}_{\underline{n}}$:

$$\hat{X}_{\underline{n}} = \prod_{\substack{n_i \in \underline{n} \\ n_i=1}} \hat{n}_i \prod_{\substack{n_i \in \underline{n} \\ n_i=0}} (1 - \hat{n}_i), \quad (7)$$

in terms of which χ can be written as

$$\chi(\underline{n}) = \sqrt{\langle \Psi | \hat{X}_{\underline{n}} | \Psi \rangle} \times (e^{iF(\underline{n})}). \quad (8)$$

Then, the ‘‘projection’’ operator $\hat{P}_{\underline{n}}$ on the fragment configuration \underline{n} is defined as:

$$\hat{P}_{\underline{n}} = \frac{\hat{X}_{\underline{n}}}{\chi(\underline{n})} = \frac{\prod_{n_i \in \underline{n}} \hat{n}_i \prod_{n_i \in \underline{n}} (1 - \hat{n}_i)}{\chi(\underline{n})} \quad (9)$$

This operator is undefined when $\chi(\underline{n}) = 0$ and we set $\hat{P}_{\underline{n}}$ to zero in that case. The action of $\hat{P}_{\underline{n}}$ on $|\Psi\rangle$ is then

$$\begin{cases} \hat{P}_{\underline{n}} |\Psi\rangle = \sum_{\underline{m}} \Phi_{\underline{n}}(\underline{m}) |\underline{n}\underline{m}\rangle & \text{if } \hat{X}_{\underline{n}} |\Psi\rangle \neq 0 \\ \hat{P}_{\underline{n}} |\Psi\rangle = 0 & \text{if } \hat{X}_{\underline{n}} |\Psi\rangle = 0 \end{cases} \quad (10)$$

and $\langle \Psi | \hat{P}_{\underline{n}}^\dagger | \Psi \rangle = \chi(\underline{n})$. This enables the writing of the embedded Hamiltonian of Eq. (6) in a very compact form:

$$h_{\underline{n}; \underline{n}'} = \langle \Psi | \hat{P}_{\underline{n}}^\dagger \hat{H} \hat{P}_{\underline{n}'} | \Psi \rangle \quad (11)$$

If it was possible to somehow obtain this embedded Hamiltonian exactly, then the exact ground-state energy of the full system could be obtained by solving the eigenproblem

$$h\chi = E\chi \quad (12)$$

in the small Hilbert space of just the fragment, regardless of how small it is, even for a single-orbital fragment!

Of course finding this Hamiltonian Eq. (11) is as difficult as solving the full problem, so an approximation enters now in the first step in our EVEF approach. We solve the HF Hamiltonian \hat{H}^{MF} for the whole system first to obtain the HF state:

$$|\Psi^{MF}\rangle = \prod_j \left(\sum_i C_{i,j} \hat{a}_i^\dagger \right) | \rangle \quad (13)$$

For a given choice of fragment \underline{n} , $\chi^{MF}(\underline{n})$ is obtained from $|\Psi^{MF}\rangle$ using Eq. (7)–(8). The advantage of the definition of Eq. (7) as a sequence of operators becomes clear now as Wick's Theorem can be used to simplify the computation of the expectation value in Eq. (8), and $\langle \Psi^{MF} | \hat{X}_{\underline{n}} | \Psi^{MF} \rangle$ becomes a sum of antisymmetrized products of one-body density matrices computed directly from $C_{i,j}$.

In the second step, the embedded Hamiltonian Eq. (11) is computed, again using Wick's Theorem. Note that the projector $\hat{P}_{\underline{n}}$ in this equation is defined using χ^{MF} . Using the resulting mean-field-derived embedded Hamiltonian

in Eq. (12) and solving it exactly (or with a high-level method) gives us directly an approximation for the total energy.

The steps above describe the central approach of this paper and it is what we call EVEF-1. This approach is expected to work well when only one subsystem (chosen as the fragment) is strongly-correlated in a bath that is well-described by a mean-field.

In the case of a large and strongly-correlated system, we instead partition the system as an ensemble of say N_f fragments, each of which is computed with a high-level method with an embedded Hamiltonian generated from HF, and combine the results. We describe this method, EVEF-2, next.

In an exact calculation, each and any fragment would correspond to a different embedded Hamiltonian in Eq. (12), denoted now \hat{h}_α where α labels the fragment, yet each would yield the same eigenvalue E , the total energy of the system. However, when an approximate Ψ is used, each fragment gives a different answer. Instead, for each fragment, one would want to separate off the part of the energy computed with the high-level method from the HF part of the energy, and sum over those parts. Let us write the total Hamiltonian in the general form:

$$\hat{H} = \sum_{i,j} t_{ij} \hat{a}_i^\dagger \hat{a}_j + \sum_{k,l,m,n} w_{klmn} \hat{a}_k^\dagger \hat{a}_l^\dagger \hat{a}_m \hat{a}_n \quad (14)$$

Then, for a fragment α in an environment consisting of the other $(N_f - 1)$ fragments, we define a ‘‘local’’ matrix h_α^{loc} , via

$$h_{\alpha;\underline{n},\underline{n}'}^{\text{loc}} = \langle \Psi | \hat{P}_{\underline{n}}^\dagger \left(\sum_{i \in \alpha, j} t_{ij} \hat{a}_i^\dagger \hat{a}_j + \sum_{k \in \alpha, l, m, n} w_{klmn} \hat{a}_k^\dagger \hat{a}_l^\dagger \hat{a}_m \hat{a}_n \right) \hat{P}_{\underline{n}'} | \Psi \rangle \quad (15)$$

which is similar to that defined in Ref. [9] for the fragment energy. The energy of the fragment is then

$$E_\alpha = \chi_\alpha^\dagger h_\alpha^{\text{loc}} \chi_\alpha \quad (16)$$

with χ_α being the solution of Eq. (12) with h_α on the left, and the total energy is obtained by repeating this over all fragments that form a full partition of the system, and summing:

$$E = \sum_{\alpha} E_\alpha \quad (17)$$

In the case no approximation is made for h_α or h_α^{loc} , this energy is exact and equal to the E appearing in Eq. (12). In fact, any observable could be obtained in a similar way.

Of course, in practise, an approximation is used, and the steps then for EVEF-2 are as follows: First, as in EVEF-1, the HF problem for the whole system is solved yielding Eq. (13), and for each fragment χ_α^{HF} is computed

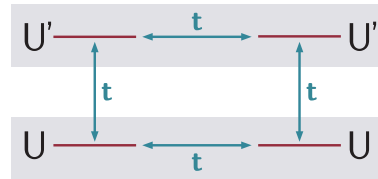


FIG. 1. Diagram of the Hubbard tetramer. In this work $t = 1/2$, $U' = 0.1$ and U is the variable.

in terms of $C_{i,j}$ in the same way. In the second step, for each fragment again as in EVEF-1, the embedded Hamiltonian h_α is computed from Eq. (11) using χ_α^{MF} in $\hat{P}_{\underline{n}}$ and the full \hat{H} , and Eq. (12) is solved for each fragment α : $h_\alpha \chi_\alpha = \hat{E} \chi_\alpha$ to find χ_α . Third, the local matrix h_α^{loc} is formed using $|\Psi^{\text{MF}}\rangle$ in Eq. (15), and the fragment energy E_α is computed from Eq. (16), and summed over all fragments as in Eq. (17).

A refinement of EVEF-2 follows from introducing a self-consistency criterium and modifying the mean field with a local or a non-local potential to fit an observable in each fragment. This is in a similar spirit to what is done in DMET and DMFT. Here, in EVEF-3, we consider only fitting the spin density. The procedure follows that of EVEF-2, but at the end of the second step, we modify \hat{H}^{HF} with a one-body term $\mu_j \hat{n}_j$, $j \in A$ to minimize $\sum_j \left\| \sum_{n_i \in \{0,1\}} |\chi(n)|^2 - |\chi^{\text{MF}}(n)|^2 \right\|$ and then iterate steps 1 and 2 until convergence is obtained.

To test our approach, we computed the energy in different Hubbard systems, with a general Hamiltonian

$$\hat{H} = - \sum_{\langle ij \rangle, \sigma} t_{ij} \hat{a}_{i,\sigma}^\dagger \hat{a}_{j,\sigma} + \sum_i U_i \hat{n}_{i,\uparrow} \hat{n}_{i,\downarrow} \quad (18)$$

There is no local potential but the on-site repulsion may vary from site to site. In cases where $\hat{P}_{\underline{n}}^\dagger | \Psi \rangle = 0$ we set $h_{\underline{n},\underline{n}'} = 0$ except when $\underline{n} = \underline{n}'$ then $h_{\underline{n},\underline{n}'} = +\infty$ (or an arbitrary large number) to prevent the lowest-energy solution being the zero eigenvalue null χ solution. Also, we set the gauge freedom $F(\underline{n})$ to zero, but a few tests with a different choice showed that it made no difference here. All units are arbitrary.

Our first system is a molecule represented by the *Hubbard tetramer* depicted in Fig. 1, with a variable on-site repulsion U on two of the sites, while the other two-sites are weakly-interacting with a fixed $U' = 0.1$. Results of EVEF-1 and EVEF-2 for the total energy E as a function of U are shown in Fig. 2.

Consider first the upper panel that corresponds to the calculation using Unrestricted HF (UHF) for Ψ^{MF} . The exact curve (black solid line) is indistinguishable from HF at small U since the total correlation from U and U' is small, and it saturates quickly for $U \approx 5$, becoming nearly constant with $E = -1.5$. UHF (blue dash-dotted) follows the same trend but saturates a little later and at higher energy, around $E = -1.38$.

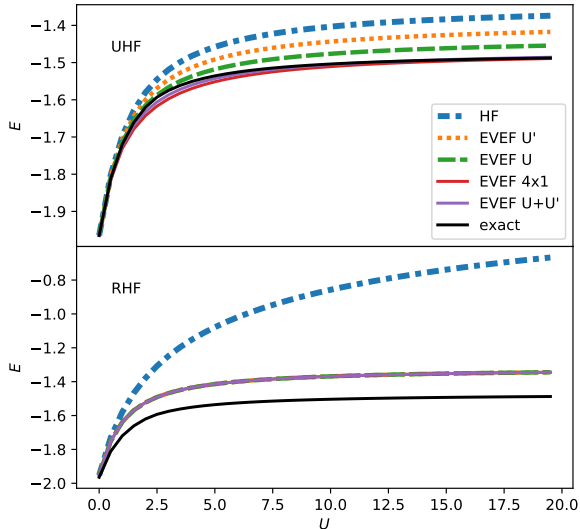


FIG. 2. Total energy E of a Hubbard tetramer as a function of U , for a HF calculation (blue dash-dotted), using EVEF-1 or EVEF-2 with fragments as indicated in the legend (see also text). Upper panel are results using UHF and lower panel are results using RHF.

The green dashed curve is the result from EVEF-1 with the natural choice of fragment being the two sites with local repulsion U . This gives a dramatic improvement over UHF for intermediate and strong correlations U . One can also make the counterintuitive choice to do the same but treating the U' part at higher level in the bath of the U sites (orange dotted line). Interestingly, this also considerably improves the energy at large U even though the correlation is almost entirely in the two sites that are *not* treated at the higher level. The effect of U is partially contained in the definition of the embedded Hamiltonian h and the ensuing diagonalization brings back some of the correlation.

The two previous fragment calculations can also be used as partition for EVEF-2 (gray rectangles in Fig.1)). Doing so gives a remarkably accurate energy (the violet solid curve), which is almost on top of the exact result. It is slightly under the exact curve in the region around $U = 5$, but as in DMET, the method is not variational so the exact energy is not a lower bound.

Another possibility for EVEF-2 is to treat each site as an independent fragment as a 4×1 partition. This is represented by the solid red curve, very close to the violet and black ones, but with a very slightly worse energy around $U = 5$.

The lower panel of Fig. 2 instead takes Ψ^{MF} as Restricted HF (RHF). In this case all EVEF (1,2,3) approaches are equivalent and, although a significant improvement over RHF is obtained especially at large U , they generate the same energy, lying between the exact

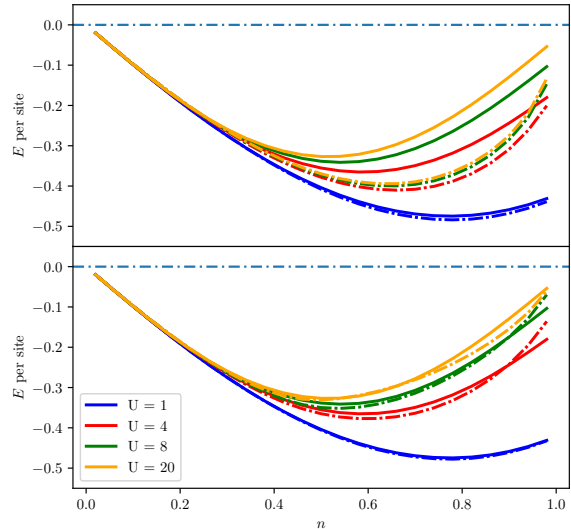


FIG. 3. Energy per site as a function of the occupation per site n in a Hubbard ring of 100 sites. Upper panel compares exact (solid) with EVEF-3 using 1-site fragment (dash-dotted), lower panel compares exact (solid) with EVEF-3 using 2-sites fragment (dash-dotted) for U -values indicated.

and RHF results. In the case of RHF, the HF determinant provides a $\chi^{HF}(n)$ which is zero for too many configurations n . Yet, some of these missing configurations n should intervene in the calculation of the exact χ . In this case, the Hilbert space in which h is actually diagonalized is too small and is the limiting factor for improvement of the energy.

Our next model system is the *uniform 100-site Hubbard ring* with $t = 1/2$ and the same U on each site. We calculate the energy from EVEF as a function of filling fraction n per site for different values of $U = 1, 4, 8, 20$ and compare with the Bethe-Ansatz solution for an infinite chain [30] as an approximately exact reference.

The results shown in Fig. 3 are from EVEF-3 using RHF as the mean-field; we found that without a chemical potential (as in EVEF-2), the number of electrons in the fragment turned out unphysical; for example, as $n \rightarrow 0$, the average number of electrons in the fragment did not go to zero. The upper panel takes the fragments to have one site while the lower panel has two-site fragments. Because of the homogeneity of the system, only one fragment calculation (one h^{loc}) needs to be done and only chemical potential μ is needed.

In both cases, EVEF-3 produces very good results for small and intermediate U , but is increasingly worse at larger U for the 1-site fragment. On the other hand, the 2-site fragment calculation greatly improves the energy, making the curve very close to the exact one even for very strong interaction strengths U . The worst results are obtained when approaching $n = 1$ where both the deriva-

tive and the value of the energy are overestimated. A similar deviation is seen in DMET calculations (Fig 1 of Ref. [8]); in fact, while DMET performs better than EVEF for one-site fragments, EVEF appears to outperform DMET for the 2-site fragment at larger U . However, since the n -site fragment calculation in DMET requires the high-level calculation in a $2n$ -site Hilbert space, then one could argue that the EVEF 2-site fragment calculation should be compared against the 1-site DMET one, and in such a comparison the errors in EVEF are much less. Calculations for a larger fragment/system size will likely improve the results further and are left for future work: our current implementation of Wick's Theorem for the matrix element needs some improvement to be more efficient. The algorithm is fully parallelizable so this will not be a limitation in future calculations.

In summary, we have derived a practical embedding method from the EF approach, establishing a new class of applications for the EF idea. EF has not previously been explored for embedding (see also Ref. [31] for an alternative EF-based embedding, that was concurrently but independently developed). The formalism can be re-cast in a numerically tractable way, thanks to Wick's theorem and is general enough that it can be applied directly to any quantum system once a basis set is chosen. We proposed three levels of refinement of this approach, EVEF-1, -2 and -3. The method produces results that are quantitatively good when tested on different Hubbard systems: a tetramer and a uniform ring, for the full range from weak to strong correlation. The accuracy is comparable to other embedding methods like DMET, and in

some cases better, but our method does not require an embedding basis (Schmidt decomposition), so the Hilbert space of the fragment in our approach is smaller. A detailed comparison with other methods and molecular or solid-state systems is left for future work, as are improvements and extensions to the EVEF approach. These include improving the stability of the self-consistency loop in EVEF-3, and choosing observables other than the local spin-density to match between the Hartree-Fock calculation and the fragment. We note that one advantage of EVEF is its flexibility as it can be used with any method that provides the expectation values needed in the definition of h . It is also not restricted to ground states, as the initial theory just starts from any eigenstate of the full Hamiltonian, thus an EVEF for excited states can be derived.

Note added: We recently became aware of work by Requist and Gross developing a similar exact factorization-based embedding method.

ACKNOWLEDGMENTS

We thank Ryan Requist for helpful discussions. Financial support from the U.S. National Science Foundation CHE-1940333 and the Department of Energy Office of Basic Energy Sciences, Division of Chemical Sciences, Geosciences and Biosciences under Award de-sc0020044 are gratefully acknowledged.

-
- [1] P. Cortona, *Phys. Rev. B* **44**, 8454 (1991).
 [2] T. A. Wesolowski and A. Warshel, *The Journal of Physical Chemistry* **97**, 8050 (1993).
 [3] A. Krishtal, D. Sinha, A. Genova, and M. Pavanello, *Journal of Physics: Condensed Matter* **27**, 183202 (2015).
 [4] S. J. R. Lee, M. Welborn, F. R. Manby, and T. F. Miller, *Accounts of Chemical Research* **52**, 1359 (2019).
 [5] A. Georges and G. Kotliar, *Phys. Rev. B* **45**, 6479 (1992).
 [6] A. Georges, G. Kotliar, W. Krauth, and M. J. Rozenberg, *Rev. Mod. Phys.* **68**, 13 (1996).
 [7] A. A. Kananenka, E. Gull, and D. Zgid, *Phys. Rev. B* **91**, 121111 (2015).
 [8] G. Knizia and G. K.-L. Chan, *Phys. Rev. Lett.* **109**, 186404 (2012).
 [9] G. Knizia and G. K.-L. Chan, *Journal of Chemical Theory and Computation* **9**, 1428 (2013).
 [10] Q. Sun and G. K.-L. Chan, *Accounts of Chemical Research* **49**, 2705 (2016).
 [11] I. W. Bulik, G. E. Scuseria, and J. Dukelsky, *Phys. Rev. B* **89**, 035140 (2014).
 [12] E. Fromager, *Molecular Physics* **113**, 419 (2015).
 [13] G. Hunter, *Int. J. Quantum Chem.* **8**, 413 (1974).
 [14] G. Hunter, *Int. J. Quantum Chem.* **9**, 311 (1975).
 [15] G. Hunter, *Int. J. Quantum Chem.* **29**, 197 (1986).
 [16] A. Abedi, N. T. Maitra, and E. K. U. Gross, *Phys. Rev. Lett.* **105**, 123002 (2010).
 [17] N. I. Gidopoulos and E. K. U. Gross, *Philosophical Transactions of the Royal Society of London A: Mathematical, Physical and Engineering Sciences* **372** (2014).
 [18] A. Abedi, N. T. Maitra, and E. K. U. Gross, *J. Chem. Phys.* **137**, 22A530 (2012).
 [19] A. Abedi, F. Agostini, Y. Suzuki, and E. K. U. Gross, *Phys. Rev. Lett.* **110**, 263001 (2013).
 [20] S. K. Min, F. Agostini, and E. K. U. Gross, *Phys. Rev. Lett.* **115**, 073001 (2015).
 [21] F. Agostini, S. K. Min, A. Abedi, and E. K. U. Gross, *Journal of Chemical Theory and Computation* **12**, 2127 (2016).
 [22] S. K. Min, F. Agostini, I. Tavernelli, and E. K. U. Gross, *The Journal of Physical Chemistry Letters* **8**, 3048 (2017).
 [23] J.-K. Ha, I. S. Lee, and S. K. Min, *The Journal of Physical Chemistry Letters* **9**, 1097 (2018).
 [24] F. Agostini and B. F. E. Curchod, *Wiley Interdisciplinary Reviews: Computational Molecular Science* **0**, e1417 (2019).
 [25] M. Filatov, S. K. Min, and C. H. Choi, *Phys. Chem. Chem. Phys.* **21**, 2489 (2019).
 [26] M. Filatov, M. Paolino, S. K. Min, and C. H. Choi, *Chem. Commun.* **55**, 5247 (2019).
 [27] A. Schild and E. K. U. Gross, *Phys. Rev. Lett.* **118**, 163202 (2017).

- [28] X. Gonze, J. S. Zhou, and L. Reining, The European Physical Journal B **91**, 224 (2018).
- [29] G. H. Gossel, L. Lacombe, and N. T. Maitra, The Journal of Chemical Physics **150**, 154112 (2019).
- [30] H. Shiba, Phys. Rev. B **6**, 930 (1972).
- [31] R. Requist and E. K. U. Gross, arXiv.